Relationship between muscle forces, joint loading and utilization of elastic strain energy in equine locomotion

Simon M. Harrison[1],*, R. Chris Whitton[2], Chris E. Kawcak[3], Susan M. Stover[4] and Marcus G. Pandy[1]

[1]Department of Mechanical Engineering, University of Melbourne, Parkville, VIC 3010, Australia, [2]Equine Centre, Faculty of Veterinary Science, University of Melbourne, Werribee, VIC 3030, Australia, [3]Gail Holmes Equine Orthopaedic Research Center, Colorado State University, CO 80523 USA and [4]JD Wheat Veterinary Orthopedic Research Lab, University of California at Davis, CA 95616, USA

*Author for correspondence (simon.m.harrison@gmail.com)

SUMMARY

Storage and utilization of strain energy in the elastic tissues of the distal forelimb of the horse is thought to contribute to the excellent locomotory efficiency of the animal. However, the structures that facilitate elastic energy storage may also be exposed to dangerously high forces, especially at the fastest galloping speeds. In the present study, experimental gait data were combined with a musculoskeletal model of the distal forelimb of the horse to determine muscle and joint contact loading and muscle–tendon work during the stance phase of walking, trotting and galloping. The flexor tendons spanning the metacarpophalangeal (MCP) joint – specifically, the superficial digital flexor (SDF), interosseus muscle (IM) and deep digital flexor (DDF) – experienced the highest forces. Peak forces normalized to body mass for the SDF were 7.3±2.1, 14.0±2.5 and 16.7±1.1 N kg^{-1} in walking, trotting and galloping, respectively. The contact forces transmitted by the MCP joint were higher than those acting at any other joint in the distal forelimb, reaching 20.6±2.8, 40.6±5.6 and 45.9±0.9 N kg^{-1} in walking, trotting and galloping, respectively. The tendons of the distal forelimb (primarily SDF and IM) contributed between 69 and 90% of the total work done by the muscles and tendons, depending on the type of gait. The tendons and joints that facilitate storage of elastic strain energy in the distal forelimb also experienced the highest loads, which may explain the high frequency of injuries observed at these sites.

Key words: musculoskeletal biomechanics, articular contact force, joint stress, carpus, fetlock injury.

INTRODUCTION

Larger animals such as ungulates and humans exhibit better locomotory efficiency than smaller animals such as mice, particularly whilst running (Heglund et al., 1982; Taylor et al., 1970). Larger animals can leverage substantial ground reaction forces (GRFs) to store strain energy in the elastic tissues of their limbs; this energy may be utilized later in the gait cycle to power body movement. Thus, storage and utilization of elastic strain energy is one means by which metabolic energy expenditure may be reduced during locomotion (Cavagna et al., 1964; Alexander, 2002). Compliant tendons also allow the leg muscles to reduce their energy expenditure by contracting isometrically under load. For example, the lateral gastrocnemius muscle remains nearly isometric during stance in the running turkey, allowing it to consume less metabolic energy than many of the other leg muscles that shorten over time (Roberts et al., 1997).

Storage and utilization of elastic strain energy is thought to be particularly significant in equine locomotion. Hyperextension of the metacarpophalangeal (MCP) joint, even in slower gaits such as walking, causes the long digital flexor tendons to stretch, resulting in the storage and release of elastic strain energy (Biewener, 1998). This mechanism is primarily responsible for the distal forelimb acting like a passive spring, allowing the animal to effectively bounce from stride to stride (Bobbert et al., 2007; McGuigan and Wilson, 2003; Witte et al., 2004). Although storage and utilization of strain energy reduces the need for more expensive muscular work (Butcher et al., 2009), it also may increase the likelihood of injury, as relatively high forces are needed to stretch the tendons and

ligaments during stance. In the horse, the tendons of the superficial digital flexor (SDF) and the interosseus muscle (IM) experience relatively large strains (Biewener, 1998; Riemersma et al., 1996), and these structures are also the ones most commonly injured (Goodship, 1993).

The forces in the flexor tendons that span the MCP joint [SDF, deep digital flexor (DDF) and IM] contribute significantly to the contact force acting at this joint (Merritt et al., 2008). As strain energy storage requires relatively high forces to be developed by the flexor tendons, the contact forces at the MCP joint must also be high, even for moderate gait speeds such as trotting (Merritt et al., 2008). Ungulates typically move at a preferred speed for each gait (Pennycuick, 1975), where the utilization of strain energy appears to be maximized. But when higher speeds are enforced, as is the case for racing horses, the considerable tendon loads resulting from strain energy storage may have deleterious effects. Joint contact forces in galloping horses have yet to be calculated, but the frequency of fatal MCP joint injuries in racehorses is known to be high (Bailey et al., 1999; Parkin et al., 2004), suggesting that at faster speeds this site may be subjected to substantial loads.

Determining muscle and joint loading *in vivo* is challenging (Merritt et al., 2010). In horses, measurements of tendon strain have been obtained by implanting strain gauge transducers directly in the tendons of live subjects (Butcher et al., 2009; Jansen et al., 1993a; Jansen et al., 1993b; Lochner et al., 1980). However, invasive experiments are limited for both ethical and practical reasons. In particular, attaching strain gauges to the tendons of a live animal is likely to affect its gait pattern (Jansen et al., 1998), and no study to

date has instrumented all of the important tendons simultaneously to record data across a wide range of gait speeds. Also, local measurements of tendon strain may not always accurately reflect the total change in length of the tendon. To our knowledge, joint contact forces in the horse have not been measured *in vivo*. Indirect methods such as musculoskeletal modeling are potentially more powerful than invasive experiments, provided the modeling results can be appropriately validated.

Accurate knowledge of individual muscle forces is needed to understand how storage and utilization of elastic strain energy promotes efficient limb movement during locomotion. Dutto et al. reported that the net work of the distal forelimb is negligible for trotting over a range of speeds (Dutto et al., 2006). Although this result suggests the existence of a mechanism for storage and utilization of strain energy, the contribution of the elastic tissues to the total work done by the lower limbs was not quantified. The proportion of the net work contributed by the utilization of strain energy has been estimated from calculations of the total work done during the gait cycle, assuming an efficiency scaled from other animals (Minetti et al., 1999) and also from estimates of tendon strain (Biewener, 1998). However, these methods do not allow estimates to be made of the relative contributions of the active and passive elements of individual muscle–tendon units to the total work done by all muscle–tendon units. Butcher et al. combined sonomicrometry measurements of muscle-fiber length with tendon strain measurements to evaluate the relative contributions of muscle and tendon work for the SDF and one portion of the DDF (Butcher et al., 2009). Their results suggest that the tendons do more work than the contractile fibers of the muscles. No study has determined the contributions of individual muscle–tendon units to the net work done by the lower-limb joints for any mode of locomotion in the horse.

Mathematical modeling is a useful tool for evaluating muscle and joint loading during movement. This approach has been used extensively to determine musculoskeletal function in human movement (Pandy and Zajac, 1991; van Soest et al., 1993; Zajac, 1993; Pandy, 2001; Shelburne et al., 2004; Shelburne et al., 2006; Pandy and Andriacchi, 2010); however, relatively few studies have applied this approach to the study of equine locomotion (Biewener, 1998; Meershoek et al., 2001; Merritt et al., 2008; Swanstrom et al., 2005a; Wilson et al., 2001). Detailed models of isolated muscle–tendon preparations have been used to study the interactions between the active and passive properties of an actuator (Swanstrom et al., 2005b), but few studies have used models of the musculoskeletal system to evaluate muscle and joint loading during gait. Biewener presented the most comprehensive model of the distal forelimb developed to date (Biewener, 1998). In that study, flexor tendon forces were calculated using only the torque developed about the carpal joint. The results showed that the strain in the DDF tendon was larger than that in the SDF tendon, contrary to findings obtained from *in vivo* strain gauge measurements (Butcher et al., 2009; Riemersma et al., 1996). Other modeling studies have produced results that agree more closely with strain gauge measurements by analyzing the torques developed about the MCP and distal interphalangeal (DIP) joints (Meershoek et al., 2001; Swanstrom et al., 2005a; Wilson et al., 2001) rather than the carpal joint, but these studies have focused only on the portion of the limb below the carpus without considering the important actions of the carpal and digital extensor muscles.

The stay apparatus of the equine forelimb, a linkage of tendons and ligaments that is thought to support the limb in standing and during locomotion, presents a number of challenges from a modeling perspective. Most notably, the two digital flexor muscle–tendon units have accessory ligaments (ALs) that generate forces in addition to the forces developed by the muscle–tendon units alone (Swanstrom et al., 2004). These ligaments insert near to the musculotendinous junction and connect the tendon to the palmar aspect of the carpus (from the DDF) or the caudal radius (from the SDF). Very few studies have considered the function of these structures (Meershoek et al., 2001; Swanstrom et al., 2005a), and a detailed mathematical model of the mechanical interactions between muscle belly, AL and the distal tendon has yet to be presented. Such a model is needed for accurate determination of the forces generated by the muscles, tendons and ligaments and for a thorough analysis of the work done by each of these structures.

The overall goal of the present study was to evaluate muscle forces, joint contact loading, and storage and utilization of elastic strain energy in the distal forelimb of the horse during overground locomotion. Our specific aims were, firstly, to identify the muscles, tendons and ligaments that develop the highest forces in walking, trotting and galloping; secondly, to identify the joints that experience the highest loads in each of these three gaits; and finally, to calculate the amount of strain energy stored and utilized in the distal forelimb as a proportion of the total work done by the muscles, tendons and ligaments. A muscle-actuated model of the distal forelimb was used to address each of these aims.

MATERIALS AND METHODS
Animals
Five horses, three quarter horses and two thoroughbreds, weighing 504.0±24.3 kg (mean ± s.d.) were used as subjects for this study. Each animal was examined by a licensed veterinary surgeon and judged to be free of obvious lameness.

Gait experiments
Two series of gait experiments were performed. The first series of experiments was conducted at the Orthopaedic Research Laboratory, Colorado State University Veterinary College of Medicine (Fort Collins, CO, USA), after approval was obtained from the institution's Animal Care and Use Committee. In these experiments, video and force plate data were recorded from the three quarter horses as each animal was led over a force platform (Bertec Corporation, Columbus, OH, USA) that was mounted flush to the ground and covered with rubber matting. Centre-of-pressure positions calculated from force plate measurements were verified under static loading conditions using a custom marker wand. The marker wand was pressed into the surface of the plate, the resulting reaction forces and moments were measured, and this information was used to compute the location of the center of pressure. These results were then verified against the positions of the centroid of the wand tip measured by a video-based motion capture system (Vicon Motion Systems, Los Angeles, CA, USA). The maximum error between the force plate and motion capture measurements was found to be 4.9 mm.

Video and force plate data were recorded for both walking and trotting. Fifteen retro-reflective markers were attached to the animal's skin and the three-dimensional locations of these markers were used to determine the position and orientation of the right distal forelimb during each gait. Three markers were placed on each of the following limb segments: hoof, pastern, metacarpus, radius and humerus. The Vicon motion capture system sampling at 60 Hz was used to track the positions of the skin markers. Ground forces were recorded at 600 Hz. For each animal, data were recorded for two trials of both walking and trotting.

The second series of experiments was conducted at Keeneland Racecourse (Lexington, KY, USA) by the University of California at Davis School of Veterinary Medicine, after approval was obtained from the institution's Animal Use and Care Advisory Committee. In these experiments, the left fore-hooves of two thoroughbred horses were fitted with a force-measuring shoe, and the horses galloped on a turf track while carrying a 67 kg rider. Details of the instrumented horseshoe are given in Roland et al. (Roland et al., 2005). Nine circular markers were painted onto the skin on the lateral aspects of the limb segments to determine the configuration of the left distal forelimb during the gallop; one marker was placed at the center of rotation of each of the following joints: the DIP joint, the proximal interphalangeal (PIP) joint and the MCP joint. Markers were also placed on the proximal third metacarpal bone (MC3), the proximal and distal radius, the distal humerus, the deltoid tuberosity of the humerus and the proximal humerus. Two retro-reflective markers were also attached to the hoof to identify the position and orientation of the instrumented shoe. Marker positions were recorded in the sagittal plane at 500 Hz using a Vicon motion capture system. Analogue data from the instrumented shoe were digitized at 1000 Hz by a computer mounted on the saddle. Each horse performed one trial of a gallop with the leading forelimb instrumented.

Raw data obtained from each experiment were filtered and resampled to ensure that the kinematic and ground force data were synchronized. The marker data from each gait trial were upsampled to the frequency of the ground force data by fitting cubic splines to the kinematic data. All data were low-pass filtered using a zero-phase-shift, second-order Butterworth filter. Marker data were filtered at 5 Hz for the walking trials and at 12 Hz for the trotting and galloping trials. Ground-force data were filtered at 50 Hz. Ground-force data from the instrumented shoe were transformed from the shoe's local reference frame to a global (inertial) reference frame using the positions of the hoof markers.

Imaging

Magnetic resonance (MR) imaging was performed on one cadaveric forelimb of a quarter horse. The limb used for imaging did not belong to one of the horses used in the gait experiments, although the mass of this animal (477 kg) was similar to the average mass of the experimental subjects. MR images were obtained from the proximal ulna down to the hoof using a 3.0 Tesla superconducting magnet and an extremity coil (Siemens, Munich, Germany). A two-dimensional, T2-weighted sequence was used to obtain transverse plane images of the bones with a field of view of 240×240 mm, an in-plane image resolution of 1 mm and an image sample depth of 2.5 mm.

Muscle, tendon, ligament and bone volumes were manually reconstructed from the MR images using a commercial image-processing software package (3D Doctor, Able Software Corp., Lexington, MA, USA). Discrete points on the centroidal paths of the muscles, tendons, and ligaments were determined from the segmented volumes. These points were transformed into a local bone-based reference frame and then incorporated into an existing musculoskeletal model of the equine forelimb (Brown et al., 2003b).
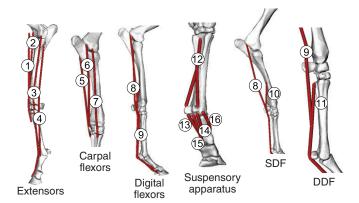
Musculoskeletal modeling

The skeleton of the distal forelimb was represented as an eight-segment, five degree-of-freedom kinematic linkage comprised of six joints: the DIP, PIP, MCP, mid-carpal (MC), antebrachiocarpal (AC) and elbow joints. The model of the DIP comprised two articulations: the distal phalanx and middle phalanx (P3–P2), and the navicular bone and middle phalanx (NB–P2). The model of the MCP was also comprised of two articulations: the proximal phalanx and third metacarpal bone (P1–MC3), and the proximal sesamoid bones and third metacarpal bone (Ses–MC3). The segments included in the model were the humerus, the radius and ulna combined, the proximal row of carpal bones, the distal row of carpal bones and the MC3 (fused at the carpometacarpal joint), the proximal phalanx (P1), the middle phalanx (P2) and the distal phalanx (P3).

The model was actuated by nine muscle–tendon units and six ligamentous structures (Fig. 1). Each muscle–tendon unit was represented as a three-element Hill-type muscle in series with an elastic tendon. The ligaments were represented as passive elastic structures. The force–length curve of each tendon and ligament was modeled by fitting a third-order polynomial function to experimental data reported in the literature (Jansen et al., 1993a; Jansen et al., 1998; Kostyuk et al., 2004; Lochner et al., 1980; Meershoek et al., 2001; Swanstrom et al., 2004; Swanstrom et al., 2005a; Swanstrom et al., 2005b; Weller, 2006). The lengths, moment arms and tendon wrapping directions of each muscle and ligament were calculated using a software program called OpenSim (Delp et al., 2007). Muscle-fiber lengths, pennation angles and physiological cross-sectional areas (PCSA) were based on data reported by Brown et al. (Brown et al., 2003a). The maximum isometric strength of each muscle was calculated from its value of PCSA by assuming a maximum isometric stress of 35 N cm^{-2} (Zajac, 1989).

Subject-specific models were created by scaling body anthropometry and the lengths and paths of the muscle–tendon units in the model to kinematic and anthropometric measurements obtained for each animal. Segmental inertial properties (i.e., mass, length, location of the center of mass and moment of inertia of each segment) were scaled to each animal's weight using regression

Fig. 1. Schematic diagram of the musculoskeletal model used in this study. The extensor muscles included in the model were the lacertus fibrosis (1), extensor carpi radialis (2), common digital extensor (3) and lateral digital extensor (4). The carpal flexor muscles included in the model were the ulnaris lateralis (5), flexor carpi ulnaris (6) and flexor carpi radialis (7). The digital flexor muscles included in the model were the superficial digital flexor (SDF; 8) and the deep digital flexor (DDF; 9). The SDF and DDF complexes included their accessory ligaments (ALs), ALSDF (10) and ALDDF (11), respectively. The suspensory apparatus comprised the interosseous muscle (IM; 12), the medial and lateral oblique sesmoidian ligaments (13 and 14) and the straight sesmoidian ligament (15). The IM was assumed to continue distally as the extensor branches (16).

equations reported by Buchner et al. (Buchner et al., 1997). The locations of the joint centers and orientations of the joint axes in the model were found by minimizing differences between the positions of surface markers located on the subject and virtual markers defined in the model (Kim et al., 2009; Reinbolt et al., 2005). Muscle–tendon lengths were scaled using ratios found by dividing inter-marker distances obtained from the kinematic measurements by inter-marker distances determined from a generic marker set defined for the model.

Calculation of musculoskeletal loading and muscle–tendon energetics

Muscle forces were found using inverse dynamics and static optimization (Anderson and Pandy, 2001). Measurements of the subject's joint motion and GRFs were input into the skeletal model. Joint angles were determined from the marker trajectories using the subject-specific rigid-body models and an inverse kinematics algorithm provided in OpenSim. Inverse dynamics was used to calculate the net moments exerted about the DIP, PIP, MCP, MC, AC and elbow joints for the stance phase of one gait cycle. The net joint moments were decomposed into individual muscle forces by solving an optimization problem that minimized the sum of the squares of the muscle activations. The optimization problem was solved subject to the physiological bounds on muscle force imposed by each muscle's force–length–velocity property (Anderson and Pandy, 2001). The forces in the accessory ligaments of the digital flexors (Fig. 2), lacertus fibrosis (LF) and the suspensory apparatus were determined by performing a series of static equilibrium analyses. Joint contact forces were found at each bone-on-bone interface by summing the separate contributions of muscle, ligament, gravitational and inertial forces calculated in the model.

Muscle (tendon) power was calculated by multiplying muscle (tendon) force by the instantaneous contraction velocity of the muscle (tendon). Muscle power was calculated separately for the contractile and parallel elastic elements of muscle. Muscle and tendon powers delivered to the skeleton were found using a computational algorithm developed by Anderson and Pandy (Anderson and Pandy, 1993). Briefly, if the velocities of the tendon and the muscle were in the same direction as the velocity of the entire muscle–tendon unit (e.g. shortening), then all of the power developed by the muscle–tendon unit was assumed to be delivered to the skeleton. If the velocities of the muscle and tendon were in opposite directions, then some of the power developed by either the muscle or tendon would be lost as heat, and the remaining power then would be delivered to the skeleton [see appendix A in Anderson and Pandy (Anderson and Pandy, 1993) for details]. Muscle (tendon) work was calculated by numerically integrating muscle (tendon) power over time.

Data analysis

Muscle forces, joint contact forces and muscle–tendon work and power were averaged across subjects for each gait. Joint contact forces were analyzed by a three-way ANOVA that included the effects of joint, gait, animal and their interactions. Muscle–tendon work was analyzed by a three-way ANOVA that included the effects of muscle–tendon component (contractile element, parallel-elastic element and tendon), gait, animal and their interactions. Joint contact forces and muscle–tendon work were log-transformed (Bland and Altman, 1996) to assess proportional changes between walking and trotting gaits. *Post hoc* comparisons were adjusted using the Sidak method. The level of significance was defined as $P<0.05$.
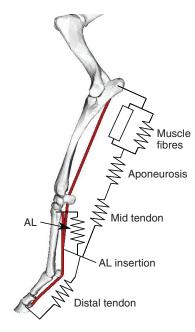

Fig. 2. Schematic diagram illustrating the model assumed for the digital flexor complexes. Both the superficial digital flexor (SDF) and deep digital flexor (DDF) muscle complexes included accessory ligaments (ALs), which are structures that insert onto the distal tendon. The diagram illustrates the model assumed for DDF. The load supported by the distal tendon was generated in part by the muscle and in part by the AL, if the latter remained taut. Each component of the flexor complex was included in the model of the muscle–tendon unit, which in turn incorporated the muscle fibre, aponeurosis, mid tendon, AL and distal tendon. Each spring in the model represented a nonlinear passive structure. The contractile element (CE) of the muscle fibres was the only component that could actively contract in the model. The location of the insertion of the AL (AL insertion) was assumed to be a function of the stiffness of the distal tendon and the combined stiffness of the AL and the proximal components of the flexor complex. See List of abbreviations for definitions.

RESULTS

The horses walked, trotted and galloped at speeds of 0.75 ± 0.05, 1.4 ± 0.1 and $6.2\pm0.6\,\mathrm{m\,s^{-1}}$, respectively. In all three gaits, the mean peak force (normalized to body mass) developed by the distal SDF tendon [muscle plus the AL of the SDF (ALSDF)] was higher than that of any other muscle or ligament in the model: 7.3 ± 2.1, 14.0 ± 2.5 and $16.7\pm1.1\,\mathrm{N\,kg^{-1}}$ in walking, trotting and galloping, respectively (Fig. 3; add forces shown for SDF and ALSDF). The mean peak force developed by the IM complex was also relatively high: 6.1 ± 1.6, 11.9 ± 2.1 and $13.1\pm0.3\,\mathrm{N\,kg^{-1}}$ in walking, trotting and galloping, respectively. The peak forces developed by the SDF and IM complexes and the muscle–tendon units of the extensor carpi radialis (ECR), flexor carpi ulnaris (FCU) and ulnaris lateralis (UL) were significantly higher in trotting than in walking ($P<0.05$, $N=3$) (Fig. 3). In late stance, the mean maximum forces transmitted by the distal DDF tendon [muscle plus the AL of the DDF (ALDDF)] in walking, trotting and galloping were 5.9 ± 1.7, 6.2 ± 2.0 and $16.1\pm6.5\,\mathrm{N\,kg^{-1}}$, respectively (Fig. 3; add forces shown for DDF and ALDDF). The carpal muscles – common digital extensor (CDE), ECR, FCU, flexor carpi radialis (FCR) and UL – were loaded mainly at the beginning and end of stance (Fig. 3). Lacertus fibrosis transmitted relatively high peak forces from the biceps complex in late stance: 2.8 ± 0.7, 2.6 ± 1.5 and $5.5\pm0.7\,\mathrm{N\,kg^{-1}}$ in walking, trotting and galloping, respectively (Fig. 3).
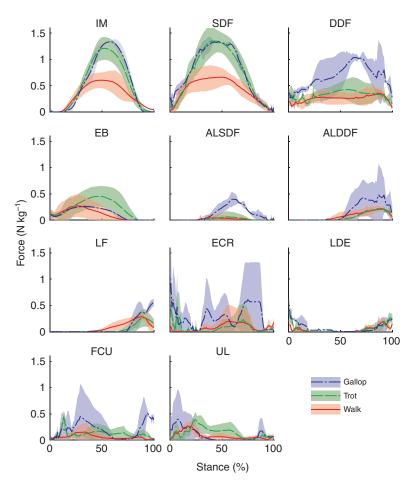
Fig. 3. Tendon and ligament forces calculated in the distal forelimb for walking (red, solid line), trotting (green dashed line) and galloping (blue dot–dash line). All forces are normalized to the mass of the whole animal, including the mass of the rider in galloping. Results are plotted as means (solid lines) ± 1 s.d. (shaded areas) (N=3 for walking and trotting; N=2 for galloping). Results for the common digital extensor (CDE) and the flexor carpi radialis (FCR) are not shown here, as the magnitudes of the forces developed by these muscles were small in comparison with those developed by the other muscles in the model. See List of abbreviations for definitions.

Peak contact forces transmitted by the MCP joint complex (P1–MC3 and Ses–MC3) were higher than those acting at the DIP joint complex (P3–P2 and NB–P2), the MC joint and the AC joint (Fig. 4). The highest peak contact force transmitted by the MCP joint during walking was 20.6±2.8 N kg^{-1} (P1–MC3). Similarly, the highest peak contact forces calculated for trotting and galloping were 40.6±9.4 N kg^{-1} (Ses–MC3) and 45.9±0.9 N kg^{-1} (P1–MC3), respectively. Joint contact loading increased significantly at all joints ($P<0.05$), except NB–P2 ($P=0.85$), as the gait transitioned from a walk to a trot (Fig. 4). The contact forces transmitted by the NB–P2 and Ses–MC3 joints were due entirely to the forces acting in the tendons. In the remaining joints, the GRF contributed at least 22% (P1–MC3) and at most 60% (P3–P2) of the peak contact force. The remainder of the contact force acting at each of these joints was contributed by tendon forces, with the highest contributions made by SDF, IM and DDF (Fig. 4).

The majority of the total work done by the distal forelimb was due to lengthening and shortening of the tendons in early and late stance, respectively (Fig. 5, Table 1). In early stance, the muscles, tendons and ligaments absorbed energy; specifically, 0.14±0.01, 0.46±0.04 and 0.24±0.04 J kg^{-1} in walking, trotting and galloping, respectively. The elastic tissues contributed 83±10, 69±16 and 90±5% of the total energy absorbed by the distal forelimb during walking, trotting and galloping, respectively. In late stance, the muscles, tendons and ligaments generated energy; specifically, 0.08±0.04, 0.24±0.10 and 0.22±0.01 J kg^{-1} during walking, trotting and galloping, respectively. The elastic tissues contributed 81±11, 86±5 and 90±7% of the total energy generated by the distal forelimb during walking, trotting and galloping, respectively. In all three gaits,

the passive elastic components of the SDF and IM complexes contributed the majority of the total work done by all the structures in the model (Fig. 5).

DISCUSSION

The overall goal of this study was to correlate muscle and joint loading with storage and utilization of elastic strain energy in the distal forelimb of the horse across a range of locomotion speeds. A muscle-actuated model of the distal forelimb was used to address the following specific aims: (1) to determine the forces developed by the muscles, tendons and ligaments during walking, trotting and galloping; (2) to identify the joint that experiences the highest load in each of these three gaits; and (3) to calculate the amount of elastic strain energy stored and utilized as a proportion of the total work done by the muscles, tendons and ligaments which actuate the distal forelimb.

To our knowledge, this is the first study to quantitatively compare the forces developed by all of the major muscles, tendons and ligaments in the lower limb of the horse across three distinct gaits: walking, trotting and galloping. We also present new information on the mechanical work done by the contractile elements and elastic tissues across the range of speeds represented by these three gaits. In particular, estimates of joint contact loading in the distal limb at a gallop have not previously appeared in the literature, and estimates of muscle contributions to the joint reaction forces have not been presented for any gait. Strain energy storage and muscle work has only been estimated for a subset of the structures of the distal limb, and muscle work has not previously been juxtaposed with magnitudes of strain energy to determine the relative contributions to the total muscle–tendon work done by the distal limb.
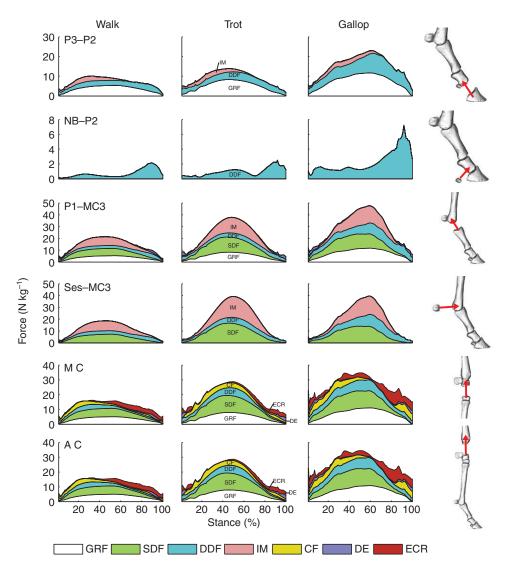
Fig. 4. Contributions of tendon, ligament and ground reaction forces to the resultant joint contact forces acting at the distal interphalangeal joint (P3–P2), the navicular bone–second phalanx contact surface (NB), the proximal phalanx–metacarpus contact surface (P1–MC3), the proximal sesamoid–metacarpus contact surface (Ses–MC3), the midcarpal joint (MC) and the antebrachiocarpal joint (AC). Forces are normalized to the mass of the whole animal, including the mass of the rider in galloping. See List of abbreviations for definitions.

The results highlight a direct link between strain energy storage in the distal limb and extreme tendon and joint-contact loading during locomotion. The structures that store the majority of strain energy, the SDF and the IM, support the highest loads, and their tendons are injured more frequently than any of the other soft tissues in the lower limb. The forces developed by the tendons of the SDF and IM contribute most significantly to the contact force transmitted by the MCP joint, which was shown to be the highest joint force acting in the distal forelimb. Not surprisingly, the MCP is also the joint at which the majority of fatal musculoskeletal injuries occur in racing horses. These deleterious effects may limit the extent to which elastic strain energy can be stored and utilized during equine locomotion. Thus, locomotory efficiency in the horse may be restricted by the magnitudes of forces to which the tendons and joints are subjected in the distal limb.

Two features of our modeling approach are also novel, particularly in their application to equine locomotion biomechanics. First, no previous model has considered the entire distal forelimb of the horse, and furthermore, the architectural properties and mechanical behavior of the carpal flexors (FCU, FCR and UL) and extensors (CDE, LDE and ECR) have not previously been included in a biomechanical model. Second, our model of the accessory ligaments of the flexor tendons is new, enabling more accurate estimates to be derived for the load sharing between the muscles, tendons and accessory ligaments in the distal limb.

Muscle, tendon and ligament loading

The model calculations showed that the SDF, IM and DDF developed the highest forces of all the muscles of the distal forelimb during walking, trotting and galloping (Table 2, Fig. 3). This is a consequence of the large torque developed about the MCP joint, which in turn results from MCP joint hyperextension. The palmar translation of the MCP joint axis that occurs during hyperextension increases the moment arm of the GRF and leads to an increase in the MCP joint torque. The length of the digit, which is comprised of the proximal, middle and distal phalanges (P1, P2 and P3), determines, for the most part, the mean moment arm of the GRF. Because the tendons of the SDF, IM and DDF are primarily responsible for supporting the MCP joint when it is subjected to an extensor torque, the forces in these tendons must increase to supply the increased joint torque. Thus, the forces in the tendons of the SDF, IM and DDF are determined mainly by the extent of MCP joint hyperextension, digit length and the magnitude of the GRF. This mechanism is similar to that found in the distal limbs of many other animals, including humans and ungulates, where the Achilles tendon force is primarily determined by ankle torque.
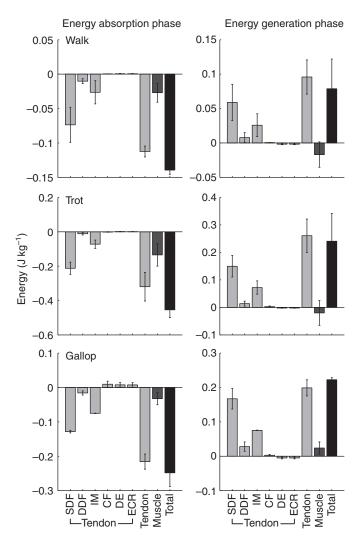
Fig. 5. Average total cumulative work done by the muscles, tendons and ligaments of the distal forelimb during the energy absorption and energy generation periods of the stance phase of gait. The energy absorption and energy generation phases constitute approximately the first half and second half of stance, respectively. Results are normalized by the mass of the whole animal, including the mass of the rider in galloping. Tendon work (light gray bars) is separated into the contributions made by the various muscle groups: SDF complex, DDF complex, IM, CF, DE and ECR. Tendon, the total work done by all the tendons and ligaments included in the model; muscle (dark gray bars) the total work done by all the muscles in the model, including SDF, DDF and IM; total (black bars), the total work done by the all the muscles, tendons and ligaments in the model. Error bars indicate 1 s.d. from the mean (N=3 for walking and trotting; N=2 for galloping). Work done by the tendons represents the majority of the total work done by the distal forelimb during each gait. The SDF and IM complexes contributed the majority of the tendon work for both the energy absorption and energy generation periods of the stance phase of each gait. See List of abbreviations for definitions.

Joint contact loading

The model calculations also showed that the combined effects of muscle forces, inertial forces and GRFs result in high contact forces transmitted by the distal joints (Fig. 4), particularly by the two articulations present at the MCP joint: the proximal phalanx to the third metacarpal bone (P1–MC3), and the proximal sesamoid to the third metacarpal bone (Ses–MC3). For all but the articulation between the distal and middle phalanges (P3–P2), tendon forces contributed the majority of the contact force acting at each joint. The major sources of joint contact loading at the MCP joint were the forces developed by the SDF and IM tendons. We note here that the GRF contributed only a small portion of the contact force acting at the P1–MC3 joint and none of the contact force acting at the Ses–MC3 joint. Because the forces in the tendons of the SDF and IM were primarily induced by extension of the MCP joint, it follows that hyperextension of the MCP joint during locomotion is the main reason why high contact forces are present at this joint.

High forces cause wear and tear of musculoskeletal tissues, increasing the risk of injury to the animal (Bennell et al., 1996; Milgrom et al., 1985; Nunamaker et al., 1991). In the horse, the structures subjected to the highest peak forces during locomotion are the MCP and carpal joints as well as the soft tissues that cross one (the IM) or both (the SDF tendon) of these joints (Figs 3 and 4). It is not surprising, therefore, that these joints and tendons are also the sites of frequent injuries observed in athletic horses (Bailey et al., 1999; Goodship, 1993; Parkin et al., 2004). It should be noted that joint stress (load per unit contact area) is a more precise indicator of possible injury than joint load. Stress analysis by finite element modeling or direct measurement is needed to determine joint stresses for the articulations of the distal limb. Gait experiments at racing speeds will need to be conducted to confirm that the MCP and carpal joints are loaded to the highest degree at the fastest galloping speeds, but it is likely that injuries to the MCP and carpal joints experienced at high speeds are a direct result of the SDF and IM tendons being subjected to very high loads.

The P3–P2 and carpal joints (AC and MC) were subjected to relatively high contact forces in the beginning and end of stance, and these forces increased with increasing speed (Fig. 4). The increased joint contact forces were caused mainly by an increase in the forces developed by the extensors [CDE, lateral digital extensor (LDE) and ECR] and carpal flexors (FCU, FCR and UL). Because muscle co-contraction increases the compressive force transmitted by a joint, this mechanism may assist in increasing joint stability (Ackland and Pandy, 2009; Andriacchi and Birac, 1993), particularly during galloping.

Storage and utilization of elastic strain energy

Our calculations of muscle, tendon and ligament work suggest that tendon work, particularly the work done by the tendons of the IM and the SDF, constitutes a clear majority of the total work done by the distal forelimb (Fig. 5). The long flexor tendons of the distal forelimb enable considerable amounts of elastic strain energy to be stored and utilized during stance. This is energetically advantageous for the animal, as stretching of the tendons presumably requires less metabolic energy to be expended by the muscles. Muscle contraction may stretch a compliant tendon, but we have calculated this effect to be relatively small (Fig. 5, Table 1). Instead, the tendons are loaded by inertial and gravitational forces when the limb is in contact with the ground. Previous studies have calculated muscle work in the hind limb of dogs (Alexander, 1974), turkeys (Roberts et al., 1997) and kangaroos (Alexander and Vernon, 1975) to be small in comparison with tendon work mainly because the muscles contract isometrically under load. By contrast, the major reason for the small magnitude of muscle work (Fig. 5, Table 1) in the equine flexor tendons is that the fibers of these muscles are much shorter than their tendons (Brown et al., 2003a). At full load, the stretch in these tendons can exceed the lengths of the fibers of the flexor muscles.

The total work done by the horse over a prescribed distance increases dramatically with speed, but the metabolic cost of locomotion does not show the same relative increase (Minetti et al.,

Table 1. Net mechanical energy absorbed and generated by the muscles, tendons and ligaments in the model during the stance phase of gait

Gait	Net mechanical energy (J kg^{-1})			
	CE	PE	Tendon	Net total
Energy absorption phase				
Walk	−0.02±0.02	0.00±0.00	−0.11±0.01	−0.14±0.01
Trot	−0.13±0.07	−0.00±0.01	−0.32±0.08	−0.46±0.04
Gallop	−0.02±0.01	−0.01±0.01	−0.22±0.02	−0.24±0.04
Energy generation phase				
Walk	−0.01±0.02	−0.01±0.00	0.10±0.02	0.08±0.04
Trot	−0.02±0.03	0.00±0.01	0.26±0.06	0.24±0.10
Gallop	0.01±0.00	0.01±0.01	0.20±0.02	0.22±0.01

The energy absorption and energy generation phases constitute approximately the first and second halves of stance, respectively.
The contributions to the total work done by the contractile elements of muscle (CE), the passive elements of muscle (PE) and tendon are presented as means ± 1 s.d. (*N*=3 for walking and trotting; *N*=2 for galloping).

1999). This result indicates that the muscles may be working more efficiently, with the tendons doing proportionately more work at the faster gaits (Biewener, 1990). Our results suggest that tendon work in trotting and galloping is much more significant than in walking (Fig. 5), but more detailed studies are needed to see if tendon work increases with speed in the faster gaits. Long tendons may have other energetic benefits for the horse because they allow for a relatively long and light distal limb, reducing the energy required for limb protraction during normal gait (Clayton et al., 2000a).

Does tendon and joint loading limit the utilization of strain energy?

Our results show that storage of elastic strain energy in the distal forelimb of the horse requires the development of high tendon forces. This finding raises new questions about the limits that tendon loading places on storage and utilization of strain energy during equine locomotion.

Does musculoskeletal loading place an upper limit on the amount of strain energy stored in the elastic tissues of the horse? The evolution of specialized long tendons and aponeuroses to store strain energy has advantages for locomotor efficiency. An increase in strain energy storage can be achieved by increasing pastern length, which would increase the moment arm of the GRF relative to the MCP joint (Biewener, 1989). However, this change would also increase the forces transmitted by the tendons and joints of the distal forelimb.

Indeed, by maintaining a more erect posture than smaller animals, large animals have adapted to minimize the moment generated by the GRF (Biewener, 1990). Hyperextension of the equine MCP joint appears to be an exception to this rule. It is likely that the equine pastern has evolved to be sufficiently long to take advantage of the benefit of strain energy storage, but sufficiently short to minimize the risk of tendon, bone and joint injury. Thus, musculoskeletal loading may not limit merely the speed of gait (Biewener and Taylor, 1986) but also the benefit that can be derived from having long, compliant tendons.

Racehorses are required to exercise regularly at high speeds during training and racing. Other domesticated horses and wild horses rarely exercise at high speeds with the same frequency. The prevalence of injury to the MCP joint and the flexor tendons is high in all horses, but it is much greater in racehorses than in wild horses and in horses used for other purposes (e.g. dressage) (Bailey et al., 1999; Cantley et al., 1999). The loads induced at these sites due to MCP extension may be manageable at low to moderate speeds and for short bursts at higher speeds, but the extreme loads generated at racing speeds are likely to put these structures at risk for fatigue failure, particularly when the animal is required to run repeatedly at high speeds over relatively long distances.

The mechanism of strain energy utilization may coincide with sports-related injuries in other animals. The Achilles tendon and the tissues in the arch of the foot contribute significantly to storage and

Table 2. Maximum forces calculated in the tendons of the distal forelimb compared to results obtained from invasive experiments reported in the literature

Gait	Tendon force (N kg^{-1})					Source
	IM	SDFT (SDF+ALSDF)	DDFT (DDF+ALDDF)	DDF	ALDDF	
Walk	6.1±1.6	7.3±2.1	5.9±1.7	3.8±1.1	2.4±0.5	Present study
Walk	−	6.73±0.57	−	1.95±0.12	−	Butcher et al., 2009
Walk	8.4±1.5	5.4±1.0	9.3±1.1	3.8±1.1	7.3±1.5	Jansen et al., 1993b
Walk	17	8	9	−	−	Lochner et al., 1980
Walk	11	9	3	−	−	Platt et al., 1994
Trot	11.9±2.1	14.0±2.5	6.2±2.0	4.9±1.3	2.4±0.6	Present study
Trot	−	11.01±0.79	−	2.81±0.18	−	Butcher et al., 2009
Gallop	13.2±0.3	16.7±1.1	16.1±6.5	11.3±0.7	5.6±4.6	Present study
Gallop	−	9.47±0.74	−	4.51±0.31	−	Butcher et al., 2009

Model and experimental data are compared for walking, trotting and galloping.
Results are presented as means ± 1 s.d. (*N*=3 for walking and trotting; *N*=2 for galloping).
All forces are normalized by the mass of the whole animal, including the mass of the rider in galloping.
ALDDF, accessory ligament of the DDF tendon; ALSDF, accessory ligament of the SDF tendon; DDF, deep digital flexor; IM, interosseous muscle; SDF, superficial digital flexor.

utilization of strain energy during running and jumping in humans (Alexander and Bennet-Clark, 1977; Anderson and Pandy, 1993; Fukashiro et al., 1995; Ker et al., 1987), and injuries to the Achilles tendon (Leppilahti and Orava, 1998) and the metatarsal bones (Pester and Smith, 1992) are common in athletes. Similarly, dogs develop large forces and store significant amounts of strain energy in their Achilles tendons (Alexander and Bennet-Clark, 1977). Canine Achilles tendons are injured due to overload events (Harasen, 2006), and racing greyhounds injure their hock (analogous to the human ankle) more often than non-racing dogs (Sicard et al., 1999). Thus, the horse may not be the only animal that benefits from storage and utilization of strain energy at moderate speeds of locomotion, while enduring a greater prevalence of soft-tissue and joint injuries in heavier exercise.

Limitations of the analysis

There are a number of limitations related to both the gait experiments performed and the model used to determine musculoskeletal loading and mechanical work done. The gait experiments were limited in at least four respects. First, the number of animals used in the experiments was small and, furthermore, the same animals were not used in all of the gait experiments. Second, because galloping is a non-symmetric gait, the leading and trailing limbs are loaded differently (Merkens et al., 1991). In particular, studies have shown that the trailing limb experiences larger GRFs than the leading limb (14.8 and 11.6 N kg^{-1}, respectively) (Merkens et al., 1991). This may explain why the model calculations showed that energy absorption in galloping was less than that in trotting. Future estimates of the work done during galloping ought to account for differences arising from limb asymmetry. Third, the speeds of gait employed were slow, and so the results may be different for faster speeds of walking, trotting and galloping. However, it is likely that the contractile elements perform more work at slower speeds, which makes our estimates of the work done appear conservative (i.e. the strain energy contributions to total work done may be larger for normal speeds of trotting and galloping). Also, the comparisons of GRFs, joint torques, joint powers, tendon forces and tendon strains (see Fig. 6 and Comparison with literature data) show that the results of this study correlate well with those reported in the literature, albeit with smaller magnitudes in some cases, reflecting the slower speeds tested here. Fourth, the galloping experiment was not conducted at racing speed, which is typically in the range of 16–18 m s^{-1} (Swanstrom et al., 2005a). It is likely that musculoskeletal loading and storage and utilization of elastic strain energy are higher than the values indicated by our results when horses gallop at their fastest speeds.

The model calculations were also limited in a number of respects. First, validation of the model was qualitative because the calculated values of tendon strains were compared against strain gauge results reported in the literature (see below). Second, the actuator lengths and material properties were obtained from the literature and were not subject-specific. Future studies should be aimed at using subject-specific material properties and geometric data to obtain the best possible estimates of muscle forces and muscle–tendon work during gait. Third, hysteresis was not included in the model used to describe the mechanical behavior of tendon. Although this effect has not been included in previous biomechanical models of equine locomotion (Meershoek et al., 2001; Swanstrom et al., 2005a), at least 7% of the total strain energy stored in the elastic tissues is estimated to be lost as heat during recoil (Ker, 1981). Fourth, static optimization was used to solve the muscle-force distribution problem in the distal limb. The static solution was constrained by the force–length–velocity property of muscle, but activation dynamics

was neglected. Anderson and Pandy compared lower-limb muscle forces obtained from static and dynamic optimization solutions of human gait and showed that muscle activation dynamics has little influence on the solution derived from static optimization (Anderson and Pandy, 2001). Finally, our model may have underestimated the magnitudes of the contact forces transmitted by the lower limb joints, particularly in the faster gaits such as galloping. The muscle-force–joint-torque redundancy problem was solved by assuming a minimum muscle activation criterion, which is analogous to minimizing muscle stress (Anderson and Pandy, 2001). It is likely that this criterion underestimates the amount of muscle co-contraction present during stance, leading to lower estimates of joint contact loading.

Comparison with literature data

Our measurements of joint angles and GRFs and our subsequent calculations of net joint torques are in general agreement with results obtained in previous studies, once differences in gait speeds are taken into account. The time histories of the joint angular displacements
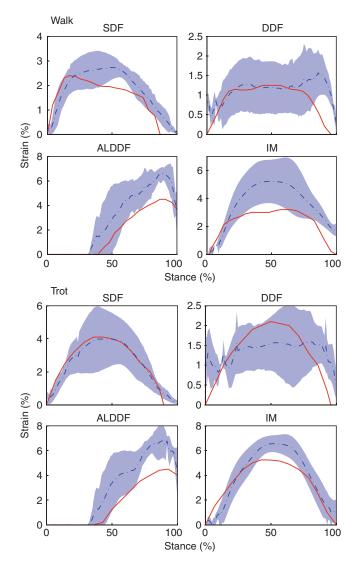

Fig. 6. Tendon and ligament strains calculated in the model. Results obtained from the model are shown as means (dashed blue lines) ± 1 s.d. (shaded areas) (N=3). The red solid lines represent strain gauge measurements reported for ponies at the walk and trot (Riemersma et al., 1996).

Table 3. Calculated values of the total amount of strain energy stored in the tendons of the distal forelimb during walking, trotting and galloping obtained in the present study compared with previously published data

| | Total amount of strain energy stored during stance (J kg⁻¹) | | | |
Gait	Distal forelimb	SDF	DDF	Source
Walk	0.11±0.01	0.07±0.03	0.01±0.00	Present study
Walk	0.03–0.06	–	–	Biewener, 1998
Walk	–	0.044±0.007	0.004±0.001	Butcher et al., 2009
Trot	0.32±0.08	0.21±0.04	0.01±0.01	Present study
Trot	0.05–0.13	–	–	Biewener, 1998
Trot	–	0.120±0.01	0.008±0.001	Butcher et al., 2009
Gallop	0.22±0.02	0.13±0.00	0.02±0.01	Present study
Gallop	0.25–0.33	–	–	Biewener, 1998
Gallop	–	0.090±0.013	0.020±0.003	Butcher et al., 2009

Results are presented as means ± 1 s.d. (N=3 for walking and trotting; N=2 for galloping).
Data are normalized to the mass of the whole animal, including the mass of the rider for galloping.
Results for Biewener (Biewener, 1998) are presented as a range: minimum–maximum.
DDF, deep digital flexor; SDF, superficial digital flexor.

measured in the present study are very similar to those reported elsewhere (Dutto et al., 2006; Clayton et al., 2000b). Peak MCP and carpal joint angles measured for trotting were 241±4 and 182±2 deg, respectively, which are similar to the values given by Clayton et al. (237.7±9.2 and 186.3±3.3 deg) (Clayton et al., 2000b). Our results for the peak vertical GRF in walking at $0.7 \, \text{m s}^{-1}$ $(5.4±0.2 \, \text{N kg}^{-1})$ compare favorably with the results of Schamhardt et al. for walking at $2 \, \text{m s}^{-1}$ $(6.8 \, \text{N kg}^{-1})$ (Schamhardt et al., 1991), particularly when the difference in walking speeds between these two studies is considered. Dutto et al. showed a strong linear dependence of forelimb vertical GRF on trotting speed (Dutto et al., 2004). The peak vertical GRF for trotting at $1.4 \, \text{m s}^{-1}$ $(8.4±0.2 \, \text{N kg}^{-1})$ found in this study is similar to that extrapolated from data reported by Dutto et al. for trotting $(8.8 \, \text{N kg}^{-1})$ (Dutto et al., 2004). We estimated the maximum torques developed about the AC, MCP and DIP joints to be 0.42±0.10, 0.53±0.03 and $0.10±0.03 \, \text{Nm kg}^{-1}$, respectively, for walking at $0.7 \, \text{m s}^{-1}$, which compare favorably with the results of Clayton et al. for walking at $1.4 \, \text{m s}^{-1}$: 0.6, 0.75 and $0.4 \, \text{Nm kg}^{-1}$ (Clayton et al., 2000a), again considering the differences in gait speeds. For trotting, we estimated the maximum torques to be 0.73±0.20, 0.93±0.14 and $0.10±0.03 \, \text{Nm kg}^{-1}$ for the AC, MCP and DIP joints, respectively, which are consistent with the results obtained by Dutto et al. for trotting at $2.5–3.25 \, \text{m s}^{-1}$: 1.0, 1.1 and $0.2 \, \text{Nm kg}^{-1}$ (Dutto et al., 2006).

Tendon and ligament strains calculated in the model are in rough agreement with results obtained from strain measurements reported in the literature. The timing and magnitudes of the model predictions agree well with the results of strain gauge experiments performed on ponies at the walk and trot (Riemersma et al., 1996) (Fig. 6). Strain magnitudes for the SDF and DDF tendons (5.0±0.5 and 3.0±1.0%, respectively) for galloping at $6.2±0.6 \, \text{m s}^{-1}$ are similar to, although larger than, the results obtained by Butcher et al. for cantering at $7.0 \, \text{m s}^{-1}$ (4.82±0.38% for the SDF tendon and 1.96±0.13% for the DDF tendon) (Butcher et al., 2009).

Direct measurements of distal tendon loads confirm that the SDF and IM experience higher forces than the other tendons of the distal forelimb during walking, trotting and galloping (Table 2). Butcher et al. determined the forces in the SDF tendon and the mid-DDF tendon from *in vivo* strain gauge experiments conducted on four horses exercising on a treadmill (Butcher et al., 2009). They assumed a linear relationship between tendon force and strain. Because our model assumed a nonlinear force–extension

relationship, it is not surprising that our calculations differ somewhat from the measurements reported by Butcher et al. (Butcher et al., 2009). Further, implantation of strain gauges can affect the gait of the animal (Jansen et al., 1998) and this may also explain the differences evident between the model and the experiment.

To our knowledge, the MCP joint contact forces obtained in the present study are the highest joint contact loads reported for any animal (Bergmann et al., 2001; Bergmann et al., 1999; Shelburne et al., 2006). When normalized to body weight, these forces are similar to the forces reported for bipeds, but higher than those reported for small quadrupeds (Bergmann et al., 1999; Page et al., 1993). We calculated 210 and 190% of body weight (10.6 and 9.7 kN, respectively) as the mean peak forces transmitted by the P1–MC3 and Ses–MC3 joints, respectively, during walking. Human hip joint forces in walking have been measured to be 238–471% of body weight (1.99–3.06 kN) (Bergmann et al., 2001; Bergmann et al., 1993), whereas knee joint forces in walking have been measured (Kim et al., 2009) and calculated (Shelburne et al., 2006) to be approximately 270% of body weight (1.75–2.02 kN). Because the contact areas in the equine MCP joint are not significantly larger than those in other species, whereas the contact forces are evidently much higher, the mean joint contact stress is likely to be much higher. For example, the joint contact area in the P1–MC3 joint under high load is approximately $450 \, \text{mm}^2$ (Brama et al., 2001) whereas the total (medial plus lateral) contact area of the human tibiofemoral joint is given to be $700 \, \text{mm}^2$ (Kettelkamp and Jacobs, 1972). Thus, the mean contact stress of the equine P1–MC3 joint can be more than 10 times higher than that estimated for the human knee in walking. Finite element analyses of the MCP joint are needed to obtain more accurate estimates of joint contact stresses in these animals.

Our estimates of strain energy in the distal forelimb for walking, trotting and galloping are similar to those reported by Biewener (Biewener, 1998) and Butcher et al. (Butcher et al., 2009) (Table 3). However, some differences are evident, which may be explained by differences in the methodologies used in these studies. First, Biewener and Butcher et al. used linear strain energy calculations that neglect the effect of the toe region of the tendon force–length curve as well as the effect of large forces at large strains. Second, their analyses did not consider the strain energy stored in the aponeuroses of the digital flexors, which we found to account for a significant portion of the total strain energy stored in the digital flexors. Third, neither of these studies

specified whether the limb from which data were collected was the leading limb during galloping. The trailing limb is loaded to a higher extent than the leading limb during a gallop (Merkens et al., 1991), but how this affects the amount of muscle work performed and the amount of strain energy stored remains unknown. Fourth, Butcher et al. did not consider the load contributed by the ALDDF (Butcher et al., 2009), which we found significantly increases the force transmitted by the distal DDF tendon (Fig. 3), thereby increasing the amount of strain energy stored in the distal forelimb. Finally, Biewener used a different method of determining muscle forces to that adopted in the present study; specifically, Biewener resolved tendon forces only from carpal torques, whereas our muscle force calculations took account of the torques developed by all the joints in the distal limb (Biewener, 1998). This difference in methodology may explain the different distribution of forces obtained for the tendons of the distal forelimb, especially in relation to the forces calculated for the IM, DDF and SDF tendons.

Other animals use significant amounts of strain energy for locomotion. As our study was confined to the distal forelimb, it is difficult to directly compare our results with those obtained for the whole animal or even the whole forelimb. Biewener and Baudinette estimated that as much as 6.4 J of strain energy is stored in the long, compliant tendons of the Tamar wallaby during ground contact (Biewener and Baudinette, 1995). When normalized by body mass, this amounts to $1.36\,\mathrm{J\,kg^{-1}}$. We estimate that $0.32\pm0.08\,\mathrm{J\,kg^{-1}}$ of strain energy can be stored in each distal forelimb of the horse during slow trotting (Table 1). Because the hind limb may store more elastic energy than the forelimb (Biewener, 1998), a more complete model of the horse is needed to obtain an accurate estimate for the whole animal. Nonetheless, if we assume that our results can be scaled to the whole body using the results of Biewener (Biewener, 1998) (i.e. that the forelimbs contribute approximately 30% of the total strain energy), then the total amount of strain energy stored for the horse is approximately $2.0\,\mathrm{J\,kg^{-1}}$ for all four limbs during a trot. This result suggests that the horse may utilize more strain energy, when normalized by body mass, than the Tamar wallaby. Other experiments have shown that up to 60% of the total limb work done by running turkeys is due to the work done by the aponeurotic part of tendon plus that done by the external tendon (Roberts et al., 1997). Our values for the proportion of work done by the distal tendons in the horse appear high in comparison to that calculated for the running turkey. However, the values for the entire equine forelimb would be lower, as our analysis excluded the large amount of work done (Dutto et al., 2006) by the muscles of the proximal limb, which have long fibers and short tendons (Payne et al., 2004; Watson and Wilson, 2007).

Conclusions

The tendons spanning the MCP joint (SDF, DDF and IM) develop the highest forces during walking, trotting and galloping; consequently, this joint is subjected to the highest loads in all three gaits. SDF, DDF and IM also contribute the majority of the total work done by the distal limb during the stance phase of walking, trotting and galloping. Thus, the tendons and joints that facilitate storage and utilization of elastic strain energy in the distal forelimb also experience the highest loads, which may explain the high frequency of injuries observed at these sites.

LIST OF ABBREVIATIONS

AC	antebrachiocarpal joint
AL	accessory ligament
ALDDF	accessory ligament of the DDF tendon
ALSDF	accessory ligament of the SDF tendon
CDE	common digital extensor
CE	contractile element of a Hill-type muscle
CF	carpal flexor muscle (FCR, FCU, UL)
DDF	deep digital flexor
DE	digital extensor muscle (CDE, LDE)
ECR	extensor carpi radialis
FCR	flexor carpi radialis
FCU	flexor carpi ulnaris
GRF	ground reaction force
IM	interosseous muscle
LDE	lateral digital extensor
LF	lacertus fibrosis
MC	midcarpal joint
MCP	metacarpophalangeal joint
MC3	third metacarpal bone
MR	magnetic resonance
NB	navicular (or distal sesamoid) bone
PCSA	physiological cross-sectional area
PE	parallel elastic element of a Hill-type muscle
P1	first (or proximal) phalanx
P2	second (or middle) phalanx
P3	third (or distal) phalanx
SDF	superficial digital flexor
Ses	proximal sesamoid bones
UL	ulnaris lateralis

REFERENCES

Ackland, D. C. and Pandy, M. G. (2009). Lines of action and stabilizing potential of the shoulder musculature. *J. Anat.* **215**, 184-197.

Alexander, R. M. (1974). The mechanics of jumping by a dog (*Canis familiaris*). *J. Zool. (Lond.)* **173**, 549-573.

Alexander, R. M. (2002). Tendon elasticity and muscle function. *Comp. Biochem. Physiol. A* **133**, 1001-1011.

Alexander, R. M. and Bennet-Clark, H. C. (1977). Storage of elastic strain energy in muscle and other tissues. *Nature* **265**, 114-117.

Alexander, R. M. and Vernon, A. (1975). The mechanics of hopping by kangaroos (Macropodidae). *J. Zool. (Lond.)* **177**, 265-303.

Anderson, F. C. and Pandy, M. G. (1993). Storage and utilization of elastic strain energy during jumping. *J. Biomech.* **26**, 1413-1427.

Anderson, F. C. and Pandy, M. G. (2001). Static and dynamic optimization solutions for gait are practically equivalent. *J. Biomech.* **34**, 153-161.

Andriacchi, T. D. and Birac, D. M. S. (1993). Functional testing in the anterior cruciate ligament-deficient knee. *Clin. Orthop. Relat. Res.* **288**, 40-47.

Bailey, C. J., Reid, S. W. J., Hodgson, D. R. and Rose, R. J. (1999). Impact of injuries and disease on a cohort of two-and three-year-old thoroughbreds in training. *Vet. Rec.* **145**, 487-493.

Bennell, K. L., Malcolm, S. A., Thomas, S. A., Wark, J. D. and Brukner, P. D. (1996). The incidence and distribution of stress fractures in competitive track and field athletes. *Am. J. Sport Med.* **24**, 211-217.

Bergmann, G., Graichen, F. and Rohlmann, A. (1993). Hip joint loading during walking and running, measured in two patients. *J. Biomech.* **26**, 969-990.

Bergmann, G., Graichen, F. and Rohlmann, A. (1999). Hip joint forces in sheep. *J. Biomech.* **32**, 769-777.

Bergmann, G., Deuretzbacher, G., Heller, M., Graichen, F., Rohlmann, A., Strauss, J. and Duda, G. N. (2001). Hip contact forces and gait patterns from routine activities. *J. Biomech.* **34**, 859-871.

Biewener, A. A. (1989). Scaling body support in mammals: limb posture and muscle mechanics. *Science* **245**, 45-48.

Biewener, A. A. (1990). Biomechanics of mammalian terrestrial locomotion. *Science* **250**, 1097-1103.

Biewener, A. A. (1998). Muscle-tendon stresses and elastic energy storage during locomotion in the horse. *Comp. Biochem. Physiol. B Biochem. Mol. Biol.* **120**, 73-87.

Biewener, A. and Baudinette, R. (1995). In vivo muscle force and elastic energy storage during steady-speed hopping of tammar wallabies (*Macropus eugenii*). *J. Exp. Biol.* **198**, 1829-1841.

Biewener, A. A. and Taylor, C. R. (1986). Bone strain: a determinant of gait and speed? *J. Exp. Biol.* **123**, 383-400.

Bland, J. M. and Altman, D. G. (1996). Statistics notes: transformations, means, and confidence intervals. *Br. Med. J.* **312**, 1079.

Bobbert, M. F., Alvarez, C. B. G., van Weeren, P. R., Roepstorff, L. and Weishaupt, M. A. (2007). Validation of vertical ground reaction forces on individual limbs calculated from kinematics of horse locomotion. *J. Exp. Biol.* **210**, 1885-1896.

Brama, P. A. J., Karssenberg, D., Barneveld, A. and van Weeren, P. R. (2001). Contact areas and pressure distribution on the proximal articular surface of the proximal phalanx under sagittal plane loading. *Equine Vet. J.* **33**, 26-32.

Brown, N. A. T., Kawcak, C. E., McIlwraith, C. W. and Pandy, M. G. (2003a). Architectural properties of distal forelimb muscles in horses, *Equus caballus. J. Morphol.* **258**, 106-114.

Brown, N. A. T., Pandy, M. G., Kawcak, C. E. and McIlwraith, C. W. (2003b). Force- and moment-generating capacities of muscles in the distal forelimb of the horse. *J. Anat.* **203**, 101-113.

Buchner, H. H. F., Savelberg, H. H. C. M., Schamhardt, H. C. and Barneveld, A. (1997). Inertial properties of Dutch warmblood horses. *J. Biomech.* **30**, 653-658.

Butcher, M. T., Hermanson, J. W., Ducharme, N. G., Mitchell, L. M., Soderholm, L. V. and Bertram, J. E. A. (2009). Contractile behavior of the forelimb digital flexors during steady-state locomotion in horses (*Equus caballus*): an initial test of muscle architectural hypotheses about in vivo function. *Comp. Biochem. Physiol. A Physiol.* **152**, 100-114.

Cantley, C. E., Firth, E. C., Delahunt, J. W., Pfeiffer, D. U. and Thompson, K. G. (1999). Naturally occurring osteoarthritis in the metacarpophalangeal joints of wild horses. *Equine Vet. J.* **31**, 73-81.

Cavagna, G. A., Saibene, F. P. and Margaria, R. (1964). Mechanical work in running. *J. Appl. Physiol.* **19**, 249-256.

Clayton, H. M., Hodson, E. and Lanovaz, J. L. (2000a). The forelimb in walking horses: 2. Net joint moments and joint powers. *Equine Vet. J.* **32**, 295-299.

Clayton, H. M., Schamhardt, H. C., Willemen, M. A., Lanovaz, J. L. and Colborne, G. R. (2000b). Net joint moments and joint powers in horses with superficial digital flexor tendinitis. *Am. J. Vet. Res.* **61**, 197-201.

Delp, S. L., Anderson, F. C., Arnold, A. S., Loan, P., Habib, A., John, C. T., Guendelman, E. and Thelen, D. G. (2007). OpenSim: open-source software to create and analyze dynamic simulations of movement. *IEEE Trans. Biomed. Eng.* **54**, 1940-1950.

Dutto, D. J., Hoyt, D. F., Cogger, E. A. and Wickler, S. J. (2004). Ground reaction forces in horses trotting up an incline and on the level over a range of speeds. *J. Exp. Biol.* **207**, 3507-3514.

Dutto, D. J., Hoyt, D. F., Clayton, H. M., Cogger, E. A. and Wickler, S. J. (2006). Joint work and power for both the forelimb and hindlimb during trotting in the horse. *J. Exp. Biol.* **209**, 3990-3999.

Fukashiro, S., Komi, P., Järvinen, M. and Miyashita, M. (1995). In vivo Achilles tendon loading during jumping in humans. *Eur. J. Appl. Physiol. Occup. Physiol.* **71**, 453-458.

Goodship, A. E. (1993). The pathophysiology of flexor tendon injury in the horse. *Equine Vet. Educ.* **5**, 23-29.

Harasen, G. (2006). Ruptures of the common calcaneal tendon. *Can. Vet. J.* **47**, 1219-1220.

Heglund, N. C. M. A., Fedak Taylor, C. R. and Cavagna, G. A. (1982). Energetics and mechanics of terrestrial locomotion. IV. Total mechanical energy changes as a function of speed and body size in birds and mammals. *J. Exp. Biol.* **97**, 57-66.

Jansen, M., van Buiten, A., van den Bogert, A. and Schamhardt, H. (1993a). Strain of the musculus interosseus medius and its rami extensorii in the horse, deduced from in vivo kinematics. *Acta Anat.* **147**, 118-124.

Jansen, M., van den Bogert, A., Riemersma, D. and Schamhardt, H. (1993b). In vivo tendon forces in the forelimb of ponies at the walk, validated by ground reaction force measurements. *Acta Anat.* **146**, 162-167.

Jansen, M. O., Schamhardt, H. C., van den Bogert, A. J. and Hartman, W. (1998). Mechanical properties of the tendinous equine interosseus muscle are affected by in vivo transducer implantation. *J. Biomech.* **31**, 485-490.

Ker, R. F. (1981). Dynamic tensile properties of the plantaris tendon of sheep (*Ovis aries*). *J. Exp. Biol.* **93**, 283-302.

Ker, R. F., Bennett, M. B., Bibby, S. R., Kester, R. C. and Alexander, R. M. (1987). The spring in the arch of the human foot. *Nature* **325**, 147-149.

Kettelkamp, D. B. and Jacobs, A. W. (1972). Tibiofemoral contact area-determination and implications. *J. Bone Joint Surg. Am.* **54**, 349-356.

Kim, H. J., Fernandez, J. W., Akbarshahi, M., Walter, J. P., Fregly, B. J. and Pandy, M. G. (2009). Evaluation of predicted knee-joint muscle forces during gait using an instrumented knee implant. *J. Orthop. Res.* **27**, 1326-1331.

Kostyuk, O., Birch, H. L., Mudera, V. and Brown, R. A. (2004). Structural changes in loaded equine tendons can be monitored by a novel spectroscopic technique. *J. Physiol.* **554**, 791-801.

Leppilahti, J. and Orava, S. (1998). Total Achilles tendon rupture: a review. *Sports Med.* **25**, 79-100.

Lochner, F., Milne, D., Mills, E. and Groom, J. (1980). In vivo and in vitro measurement of tendon strain in the horse. *Am. J. Vet. Res.* **41**, 1929-1937.

McGuigan, M. P. and Wilson, A. M. (2003). The effect of gait and digital flexor muscle activation on limb compliance in the forelimb of the horse *Equus caballus. J. Exp. Biol.* **206**, 1325-1336.

Meershoek, L. S., van den Bogert, A. J. and Schamhardt, H. C. (2001). Model formulation and determination of in vitro parameters of a noninvasive method to calculate flexor tendon forces in the equine forelimb. *Am. J. Vet. Res.* **62**, 1585-1593.

Merkens, H. W., Schamhardt, H. C., Van Osch, G. J. V. M. and van den Bogert, A. J. (1991). Ground reaction force analysis of Dutch warm blood horse at canter and jumping. *Equine Exerc. Physiol.* **3**, 128-135.

Merritt, J. S., Davies, H. M. S., Burvill, C. and Pandy, M. G. (2008). Influence of muscle-tendon wrapping on calculations of joint reaction forces in the equine distal forelimb. *J. Biomed. Biotechnol.* **2008**, 165730.

Merritt, J. S., Pandy, M. G., Brown, N. A. T., Burvill, C. R., Kawcak, C. E., McIlwraith, W. and Davies, H. M. (2010). Mechanical loading of the distal end of the third metacarpal bone in horses during walking and trotting. *Am. J. Vet. Res.* **71**, 508-514.

Milgrom, C., Giladi, M., Stein, M., Kashtan, H., Margulies, J. Y., Chisin, R., Steinberg, R. and Aharonson, Z. (1985). Stress fractures in military recruits. A prospective study showing an unusually high incidence. *J. Bone Joint Surg. Br.* **67B**, 732-735.

Minetti, A. E., ArdigO, L. P., Reinach, E. and Saibene, F. (1999). The relationship between mechanical work and energy expenditure of locomotion in horses. *J. Exp. Biol.* **202**, 2329-2338.

Nunamaker, D. M., Butterweck, D. M. and Black, J. (1991). In vitro comparison of thoroughbred and standardbred racehorses with regard to local fatigue failure of the third metacarpal bone. *Am. J. Vet. Res.* **52**, 97-100.

Page, A. E., Allan, C., Jasty, M., Harrigan, T. P., Bragdon, C. R. and Harris, W. H. (1993). Determination of loading parameters in the canine hip in vivo. *J. Biomech.* **26**, 571-579.

Pandy, M. G. (2001). Computer modeling and simulation of human movement. *Annu. Rev. Biomed. Eng.* **3**, 245-273.

Pandy, M. G. and Andriacchi, T. P. (2010). Muscle and joint function in human locomotion. *Annu. Rev. Biomed. Eng.* **12**, 401-433.

Pandy, M. G. and Zajac, F. E. (1991). Optimal muscular coordination strategies for jumping. *J. Biomech.* **24**, 1-10.

Parkin, T. D. H., Clegg, P. D., French, N. P., Proudman, C. J., Riggs, C. M., Singer, E. R., Webbon, P. M. and Morgan, K. L. (2004). Risk of fatal distal limb fractures among thoroughbreds involved in the five types of racing in the United Kingdom. *Vet. Rec.* **154**, 493-497.

Payne, R. C., Veenman, P. and Wilson, A. M. (2004). The role of the extrinsic thoracic limb muscles in equine locomotion. *J. Anat.* **205**, 479-490.

Pennycuick, C. J. (1975). On the running of the gnu (*Connochaetes taurinus*) and other animals. *J. Exp. Biol.* **63**, 775-799.

Pester, S. and Smith, P. C. (1992). Stress fractures in the lower extremities of soldiers in basic training. *Orthop. Rev.* **21**, 297-303.

Platt, D., Wilson, A. M., Timbs, A., Wright, I. M. and Goodship, A. E. (1994). Novel force transducer for the measurement of tendon force in vivo. *J. Biomech.* **27**, 1489-1493.

Reinbolt, J. A., Schutte, J. F., Fregly, B. J., Koh, B. I., Haftka, R. T., George, A. D. and Mitchell, K. H. (2005). Determination of patient-specific multi-joint kinematic models through two-level optimization. *J. Biomech.* **32**, 621-626.

Riemersma, D., van den Bogert, A., Jansen, M. and Schamhardt, H. (1996). Tendon strain in the forelimbs as a function of gait and ground characteristics and in vitro limb loading in ponies. *Equine Vet. J.* **28**, 133-138.

Roberts, T. J., Marsh, R. L., Weyand, P. G. and Taylor, C. R. (1997). Muscular force in running turkeys: the economy of minimizing work. *Science* **275**, 1113-1115.

Roland, E. S., Hull, M. L. and Stover, S. M. (2005). Design and demonstration of a dynamometric horseshoe for measuring ground reaction loads of horses during racing conditions. *J. Biomech.* **38**, 2102-2112.

Schamhardt, H. C., Merkens, H. W. and Van Osch, G. J. V. M. (1991). Ground reaction force analysis of horses ridden at the walk and trot. *Equine Exerc. Physiol.* **3**, 120-127.

Shelburne, K. B., Pandy, M. G., Anderson, F. C. and Torry, M. R. (2004). Pattern of anterior cruciate ligament force in normal walking. *J. Biomech.* **37**, 797-805.

Shelburne, K. B., Torry, M. R. and Pandy, M. G. (2006). Contributions of muscles, ligaments, and the ground-reaction force to tibiofemoral joint loading during normal gait. *J. Orthop. Res.* **24**, 1983-1990.

Sicard, G. K., Short, K. and Manley, P. A. (1999). A survey of injuries at five greyhound racing tracks. *J. Small Anim. Pract.* **40**, 428-432.

Swanstrom, M. D., Stover, S. M., Hubbard, M. and Hawkins, D. A. (2004). Determination of passive mechanical properties of the superficial and deep digital flexor muscle-ligament-tendon complexes in the forelimbs of horses. *Am. J. Vet. Res.* **65**, 188-197.

Swanstrom, M. D., Zarucco, L., Hubbard, M., Stover, S. M. and Hawkins, D. A. (2005a). Musculoskeletal modeling and dynamic simulation of the thoroughbred equine forelimb during stance phase of the gallop. *J. Biomech. Eng.* **127**, 318-328.

Swanstrom, M. D., Zarucco, L., Stover, S. M., Hubbard, M., Hawkins, D. A., Driessen, B. and Steffey, E. P. (2005b). Passive and active mechanical properties of the superficial and deep digital flexor muscles in the forelimbs of anesthetized Thoroughbred horses. *J. Biomech.* **38**, 579-586.

Taylor, C. R., Schmidt-Nielsen, K. and Raab, J. L. (1970). Scaling of energetic cost of running to body size in mammals. *Am. J. Physiol.* **219**, 1104-1107.

van Soest, A. J., Schwab, A. L., Bobbert, M. F. and van Ingen Schenau, G. J. (1993). The influence of the biarticularity of the gastrocnemius muscle on vertical-jumping achievement. *J. Biomech.* **26**, 1-8.

Watson, J. C. and Wilson, A. M. (2007). Muscle architecture of biceps brachii, triceps brachii and supraspinatus in the horse. *J. Anat.* **210**, 32-40.

Weller, R. (2006). The influence of conformation on locomotor biomechanics and its effect on performance in the horse, PhD Thesis 2006, The Royal Veterinary College, University of London.

Wilson, A. M., McGuigan, M. P., Su, A. and van den Bogert, A. J. (2001). Horses damp the spring in their step. *Nature* **414**, 895-899.

Witte, T. H., Knill, K. and Wilson, A. M. (2004). Determination of peak vertical ground reaction force from duty factor in the horse (Equus caballus). *J. Exp. Biol.* **207**, 3639-3648.

Zajac, F. E. (1989). Muscle and tendon: properties, models, scaling, and application to biomechanics and motor control. *Crit. Rev. Biomed. Eng.* **17**, 359-411.

Zajac, F. E. (1993). Muscle coordination of movement: a perspective. *J. Biomech.* **26**, 109-124.